Biol. Cybern. 74, 299–308 (1996)

Biological Cybernetics

On the complex dynamics of intracellular ganglion cell light responses in the cat retina

A. W. Przybyszewski[1], M. J. M. Lankheet[2], W. A. van de Grind[2]

[1] Department of Cognitive and Neural Systems, Boston University, Boston, MA 02215, USA
[2] Helmholtz Institute and Department of Comparative Physiology, Utrecht University, Padualaan 8, NL-3584 CH Utrecht, The Netherlands

Received: 25 October 1994 / Accepted in revised form: 19 September 1995

Abstract. We recorded intracellular responses from cat retinal ganglion cells to sinusoidal flickering lights, and compared the response dynamics with a theoretical model based on coupled nonlinear oscillators. Flicker responses for several different spot sizes were separated in a "smooth" generator (G) potential and corresponding spike trains. We have previously shown that the G-potential reveals complex, stimulus-dependent, oscillatory behavior in response to sinusoidally flickering lights. Such behavior could be simulated by a modified van der Pol oscillator. In this paper, we extend the model to account for spike generation as well, by including extended Hodgkin-Huxley equations describing local membrane properties. We quantified spike responses by several parameters describing the mean and standard deviation of spike burst duration, timing (phase shift) of bursts, and the number of spikes in a burst. The dependence of these response parameters on stimulus frequency and spot size could be reproduced in great detail by coupling the van der Pol oscillator and Hodgkin-Huxley equations. The model mimics many experimentally observed response patterns, including non-phase-locked irregular oscillations. Our findings suggest that the information in the ganglion cell spike train reflects both intraretinal processing, simulated by the van der Pol oscillator, and local membrane properties described by Hodgkin-Huxley equations. The interplay between these complex processes can be simulated by changing the coupling coefficients between the two oscillators. Our simulations therefore show that irregularities in spike trains, which normally are considered to be noise, may be interpreted as complex oscillations that might carry information.

1 Introduction

1.1 Extracting information from noisy spike trains by applying averaging methods

The spontaneous activity of most structures in the central nervous system (CNS) is irregular. In the past, periodic stimulation and averaging techniques have been used to remove these irregularities from the response. This approach assumes that the spike train consists of separable signal and noise components. By repeating the same stimulus many times and averaging, the signal-to-noise ratio can be improved (e.g., de Boer and Kuyper 1968). In this approach, averaging serves to separate signal from stochastic fluctuations.

Despite their elegance, there are several limitations to averaging techniques in electrophysiology. The temporal resolution of averaging is often too coarse to represent the changes introduced by fast adaptation processes. More importantly, many neuronal structures show response regularities that are not phase-locked and would go unnoticed in averaged responses. In the retina, for example, responses to diffuse light flashes show multiresolution oscillations, which may or may not be phase-locked to the stimulus (Przybyszewski 1991). Rather than assuming a stimulus-locked signal and irrelevant noise, we propose to describe the dynamics of ganglion cell responses as resulting from the interplay between several different dynamical processes.

We use intracellularly recorded ganglion cell responses in the cat retina as an example because they reveal both the generator potential and the generated spikes, and thus allow intraretinal processing and spike generation to be studied in great detail. To analyze intraretinal processing and spike generation separately, the intracellular potential can be separated into a slow generator potential and a train of fast action potentials. In a previous paper (Przybyszewski et al. 1993), we analyzed the dynamics of the generator potential responses. It was shown that the generator potential consists of highly complex oscillations which are not necessarily phase-locked to the light stimulus. By changing flicker frequency or spot size, for example, the generator potential oscillations could be changed from synchronized to non synchronized and vice versa. In contrast, other components of the ganglion cell responses were always synchronized to the stimulus. These synchronized responses account for the fact that averaging or post-stimulus-time histogram (PSTH) techniques can be used to extract information under most circumstances. However, they do not reveal all the information present in the response.

To the memory of Prof. Otto-Joachim Grüsser

Correspondence to: A.W. Przybyszewski, Center for Adaptive Systems, Boston University, 677 Beacon Street, Boston, MA 02215, USA

0.1 Noise and spontaneous oscillations

Like most other cells in the CNS, cat retinal ganglion cells typically show a characteristic spontaneous activity. Spontaneous activity can be interpreted as intrinsic oscillatory behavior in the CNS. Such spontaneous oscillations complicate neural responses to even very simple stimuli, because interactions occur between the response to the stimulus and the intrinsic oscillations. In our previous paper we modeled such interactions in the generator potential of cat retinal ganglion cells using the Bonhoeffer–van der Pol oscillator (Przybyszewski et al. 1993). The work presented in this paper is an extension of the previous analysis of ganglion cell responses. Here, we also consider cell membrane properties and simulate spike train responses to sinusoidally modulated light spots. The resulting model allows us to describe seemingly irregular spike responses as complex, deterministic oscillations. Since we describe both the generator potential responses and spike generation, we can correlate different types of oscillation in the spike train with different underlying processes: intraretinal processes determining the generator potential and membrane properties responsible for spike generation. We will show that the real-time, complex dynamics of the generator potential and spike train responses can result from the interplay between these processes.

0.2 The dynamical systems approach to neural signal dissection

The interaction between different parts of the CNS, and between the generator potential and membrane channels, can be generalized to a coupling between different oscillators. Cowan and Wilson (1972) proposed dividing the CNS into inhibitory and excitatory neuronal populations with mutual coupling between them. This approach was later applied to different parts of the brain and extensively used for the olfactory system (Baird 1986; Freeman 1987). Freeman (1987) modeled the olfactory system with coupled masses of excitatory-inhibitory neurons on different levels, from receptor to cortex, and compared his simulations to electroencephalographic (EEG) experimental results. He found similarities between experimentally observed attractors and attractors in his model. Baird (1986) used a similar model to construct a unified theory of pattern recognition and associative memory. This work provided a new understanding of many neurophysiological mechanisms and showed the merit of a dynamical systems approach to neurophysiology.

In this study we investigate the usefulness of this approach for the activity at the level of ganglion cells in the cat retina. From a mathematical point of view, a general theoretical analysis of the behavior of multiple, coupled oscillators is difficult (Baesens et al. 1991; Linsay and Cumming 1989). Very complex behaviors, such as quasi-periodicity or chaos, are natural for such systems. This kind of irregularity is difficult to differentiate from noise under experimental conditions. Experimentally, the approach involves identifying points of bifurcation by changing experimental parameters and comparing them with proposed theoretical models (Aguirre and Billings 1994). We used such an approach to identify invariants in the spike train which cannot be found by using only time or frequency averaging methods. The resulting model allows us to describe seemingly irregular spike responses as complex, deterministic oscillations. The analysis furthermore shows which local retinal oscillations are being transmitted in the spike train, and which part of the activity results from processes related to spike generation.

1 Methods

1.1 Data recording

The methods of animal preparation and intracellular recording have been described in detail before (van de Grind 1981; Lankheet et al. 1989; Przybyszewski et al. 1993). Experiments were performed with the animals (cats) under pentobarbital anesthesia (40 mg/kg i.p. initial dose). The cats were artificially ventilated and end-tidal PCO_2 was kept between 3.5% and 4.5%. Muscle relaxation was initiated with 80 mg flaxedil and maintained with a continuous infusion of 6.6 mg gallamine triethiodide, 0.25 mg *d*-tubocurarine, and 5% glucose in 3 ml Ringer solution per hour per kilogram b.w. The form of the intra-aortic electrocardiogram (EKG), the stability of the heart rate, and blood pressure were monitored throughout the procedure. These data were used to dose additional i.v. injections of pentobarbital during the experiment. Rectal temperature was kept at approximately 38 °C. Pupils were dilated with atropine, and phenylephrine was used to retract the nictitating membrane. Lidocaine 2% was injected at all surgical sites.

Ganglion cell activity was recorded intracellularly in the optically intact *in situ* eye. Cells were classified on the basis of their responses to light flashes of 2 s duration and a spot diameter approximately equal to the size of the receptive field center. A cell was called "sustained" or X-type (Enroth-Cugell and Robson 1966) if there was a significant difference in spike frequency between the end of the stimulation period and the return to baseline activity. The light spots were centered on the receptive field and were either sinusoidally or square-wave modulated in intensity. We recorded responses as a function of temporal frequency for several different spot sizes. The mean luminance was in the photopic range (53–530 cd/m^2). The modulation depth was 0.6 in all cases. The data were sampled with 16-bit resolution at a frequency of 10 kHz.

1.2 Data analysis

Intracellularly recorded ganglion cell activity consists of a "slow" generator potential and fast, superimposed spikes. These two response components were separated using wavelet functions to identify spikes and spline approximations to estimate the spike-free generator potential. These procedures have been fully described in previous papers (Przybyszewski 1991; Przybyszewski et al. 1993). The resulting spike trains were then analyzed by comparing responses in each stimulation period. All responses consist of clearly recognizable spike bursts separated by silent periods (Fig. 3). A spike burst was defined as a group of spikes separated by the longest silent period in each stimulus cycle. Each response cycle thus contains a single spike burst and a silent period. The spike bursts can be regular or irregular over many repeated stimulus cycles, and they can differ in duration relative to the silent periods. To compare the experimental spike trains with model simulations, we quantified the spike responses by the following parameters:

- Mean, relative burst duration, T_d/T_p, where T_d is the duration of a spike burst and T_p the silent period between bursts.
- Mean phase, ϕ, describing the position of the spike burst relative to the stimulus. It is defined as the phase difference between the beginning of spike discharges and the minimum intensity in each stimulus cycle.
- The irregularity, σ_r, of spike burst duration over successive stimulus periods. It is defined as the standard deviation of the relative burst duration, divided by the mean T_d/T_p, σ_r is equivalent to the normalized standard deviation.
- The mean number of spikes, n, in each period of stimulation.

Together, these parameters capture the most important features of the different patterns observed in responses to sinusoidally flickering lights, for different spot sizes. The response parameters were calculated over four consecutive stimulus periods. The first several periods of stimulation were discarded to exclude the initial transients in the responses. In some cases we observed response modulations much slower than the frequency of stimulation (e.g. Fig. 3A; spot size 0.5 deg and frequency 8 Hz). In such cases we started the analysis after the infrequent irregularities. The parameters were calculated for both the experimental responses and the simulated model responses in exactly the same way and for the same number of periods.

1.3 Simulations

Our model takes the form of a set of nonlinear differential equations that describe the generator potential and membrane properties. Simulations were performed on a Sun Workstation using a modified Dynamical Systems Toolkit (dstool) with an Interactive Graphical Interface (Back et al. 1992). Integrations were performed using the Runge-Kutta method for a relatively small time step (0.01–15 μs). The model simulates the intracellularly recorded membrane potentials, consisting of a slow generator potential with superimposed fast spikes. These simulated model responses were analyzed in the same manner as were the experimental data.

2 Results

We will first describe the experimental results on spike activity. The spike trains contain all the information available to the higher visual centers. This is also the only information that could be obtained by extracellular measurements. Next, we will show how these spike trains result from interactions between intracellular generator potentials and spike generation processes. To this end, we will briefly summarize the description of generator potential dynamics in terms of a modified van der Pol equation (see Przybyszewski et al. 1993, for more details); then we outline the Hodgkin-Huxley equations describing active membrane properties responsible for spike generation; and finally we describe their interaction, by coupling the van der Pol oscillator and Hodgkin-Huxley equations to show how different modes of oscillatory activity can be simulated by changing the strength of coupling.

2.1 Spike train properties as a function of stimulus frequency

In a previous paper we have given a qualitative description of ganglion cell responses to sinusoidal flicker, for different spot sizes and flicker frequencies (Przybyszewski et al. 1993). Here we give a quantitative description of the spike train, using the parameters summarized in the Methods section. All experimental data that we show are from a single, extraordinarily stable, and long-lasting recording. Note that it was not our objective to provide a detailed comparison of parameter values between different recordings. The data set for this cell served as a representative example, and we used it to illustrate the principles of the analysis. The cell was classified as an on-center, X-type ganglion cell. It had a receptive field of 0.7 deg diameter, at about 3 deg eccentricity.

Figure 1A shows the relative burst duration, T_d/T_p, as a function of the stimulation frequency for spot diameters of 0.7, 0.5 and 0.2 deg. Simulation results for all spot sizes and stimulation frequencies (see below) are included for comparison. The functions are nonlinear for all spot sizes and reach a minimum around 8 Hz. At this frequency the burst duration for spot sizes of 0.7 and 0.5 deg is very short. The change of burst duration with frequency clearly differs for different spot sizes. For a spot of 0.7 deg, T_d/T_p changes by about a factor of 50 for modulation frequencies between 2 and 8 Hz. For smaller spots (0.2 deg), the influence of frequency on burst duration is significantly weaker, and the function is almost flat.

Figure 1B shows the phase lag, ϕ, between the stimulus and beginning of the spike bursts, also as a function of flicker frequency, and with spot size as the parameter in the graph. The phase lag increases linearly with frequency and there is no difference between these functions for different spot sizes. Such a linear phase-frequency relationship could also be described as a fixed time delay between the stimulus and the beginning of a burst. The slope of the curves in Fig. 1B would correspond to a delay of 50–80 ms.

Figure 1C shows the irregularity of burst duration, σ_r, as a function of stimulation frequency. A decrease in spot size from 0.7 deg to 0.5 deg causes a strong (3- to 10-fold) increase of the irregularity measure σ_r. A further decrease in spot size from 0.5 to 0.2 deg has relatively little influence on the irregularity of burst duration. Spike bursts are extremely regular for a stimulation frequency of 8 Hz and for a spot size of 0.7 deg. This is also clearly illustrated in Fig. 3, in which traces of the intracellular responses are presented. A decrease or increase of flicker frequency caused an increase in irregularity (by a factor of 10 in some cases) relative to a frequency of 8 Hz.

In Fig. 1D, the mean number of spikes per stimulus period, n, is plotted as a function of the stimulation frequency. For all spot sizes the number of spikes decreases monotonically with temporal frequency. The influence of spot size is negligible.

In summary, the response parameters in Fig. 1 provide a quantitative description of the different spike patterns that were experimentally observed for different flicker frequencies and for different spot sizes. The mean burst duration and regularity of burst duration show a strong dependence on spot size, whereas phase shift and the number of spikes per period do not.

2.2 Analysis and simulation of the generator potential

In a previous paper we analyzed and modeled the dynamics of the generator potential, after removal of the spikes from the intracellularly recorded responses. A wavelet method and spline interpolation of the "spike scars" was used to reconstruct a spike-free generator (G-) potential (Przybyszewski 1991). We used the pseudo-phase space with van der Pol transformation (Przybyszewski et al. 1993) to show how oscillations in the G-potential are synchronized with the stimulus. In three-dimensional phase space the generator potential shows two different oscillations: one with a period equal to the stimulus period and a second, faster one which appears only during part of a stimulation period. The faster oscillations are not exactly synchronized with the stimulus,

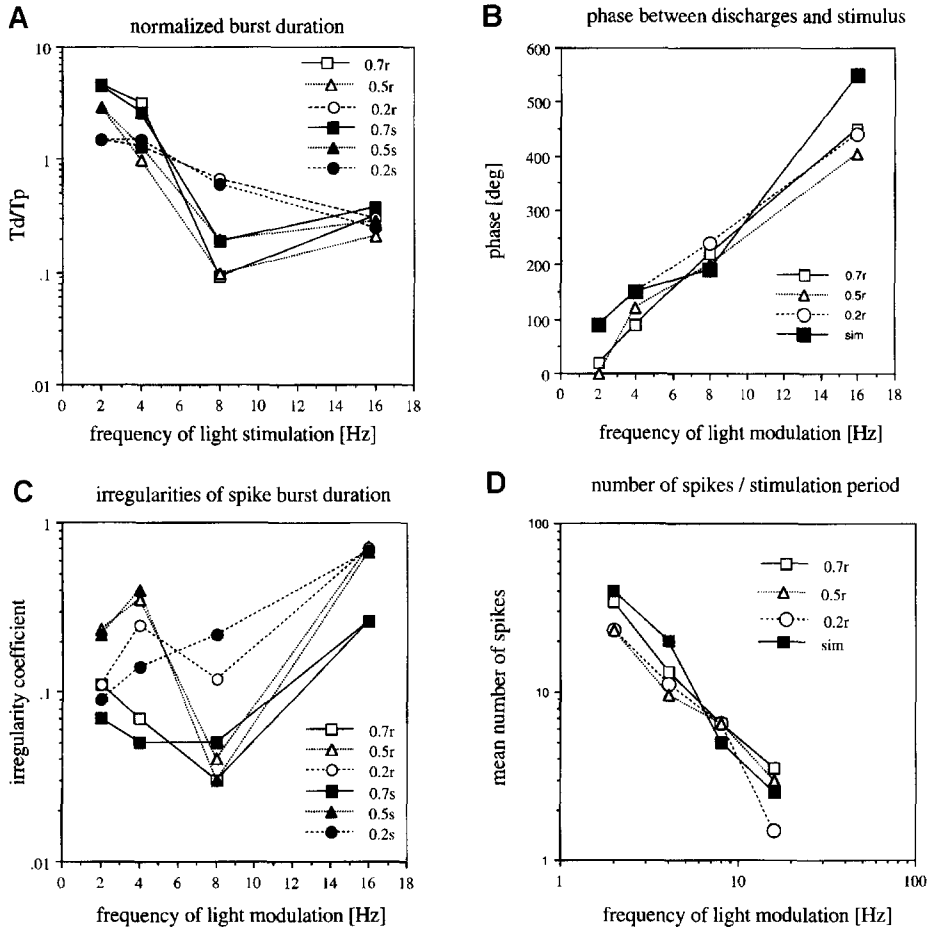

Fig. 1A–D. Experimental and simulation results for the different parameters describing the spike bursts as a function of flicker frequency. The stimulus parameter in each graph is the spot size, given in degrees; r stands for experimental recordings and s for simulated results. The results for different spot sizes in **B** and **D** could be simulated with the same model coefficients

but all appear around the same phase of the slower oscillations. This characteristic behavior was observed for many different frequencies of stimulation and different spot sizes (Przybyszewski et al. 1993).

To simulate the oscillations in the G-potential we used the Bonhoeffer–van der Pol differential equation:

$$\frac{dx}{dt} = k(y + x - x^3/3) \tag{1a}$$

$$\frac{dy}{dt} = 1/k(-x + a + b\cos(\omega t)) \tag{1b}$$

where: k is a positive constant which determines the nonlinearity, b is the amplitude of the forcing term, $\omega = 2\pi f$, f being the frequency of the forcing signal, and a is a constant threshold for the external forcing signal.

In phase space, the flow spends most of the time near a stable manifold of the lower branch of the curve: $y = -x + x^3/3$. There is a critical value of parameter a and the forcing term amplitude, for which the solution $x(t)$ enters an unstable region, and a Hopf bifurcation occurs (Honerkamp et al. 1985). When the flow approaches an unstable branch, relaxation oscillations take place. These can be seen as fast oscillations in part of the slow oscillation period. By changing the parameter a, the equilibrium point of the system will change and the phase of the stimulation period where the Hopf bifurcation occurs can be changed, leading to a transition from a stable equilibrium to a stable limit cycle (Braaksma 1993).

The critical stimulation frequency in our experimental data was 8 Hz. It represents the most nonlinear case, with only one period of the fast oscillations occurring in each stimulus period. A decrease of the stimulation frequency from 8 Hz to 4 Hz and to 2 Hz increases the number of fast oscillations in every period of stimulation. Changing the stimulation frequency also changed the synchronization of the fast oscillations relative to the slow oscillations. For flicker frequencies of 8 Hz and 4 Hz, the two types of oscillation are synchronized, whereas for a frequency of 2 Hz we observed quasi-periodicity. All these different response patterns could be simulated with the van der Pol oscillator. The critical parameter for reproducing the previously described changes in the generator potential was the coefficient of nonlinearity, k. In the most nonlinear case (8 Hz), k had a value of 4. Response patterns at higher frequencies (16 and 24 Hz) were well reproduced with a value for k of about 2, whereas for lower frequencies a value of about 3 was optimal.

By modeling the generator potential with the van der Pol oscillator we summarize all intraretinal information processing that underlies the responses in a simple set of differential equations. The van der Pol oscillator thus serves as a black box description of many different processes that finally result in modulations of the G-potential of ganglion cells. The striking similarities between the simulated and experimental response patterns show that the system can be characterized mathematically as an externally forced nonlinear oscillator.

The G-potential shows all the information available before the signal is converted into a spike train. However, higher visual centers and most electrophysiologists have available only the information present in the spike train. In this light it is more interesting, therefore, to know what information is passed on from the G-potential to the spike train, and how the different response patterns can be observed in spike trains. To answer this question we extend the analysis in the next section to include spike generation. Spike generation will be described by Hodgkin-Huxley equations based on patch-clamp recordings from cat and rat retinal ganglion cells.

2.3 Membrane properties and spike generation

Patch-clamp recordings from enzymatically dissociated solitary cat and rat retinal ganglion cells revealed that the cell membrane contains multiple types of voltage-activated ion channels (Lipton and Tauck 1987; Kaneda and Kaneko 1991a,b; Skaliora et al. 1993). These voltage-gated channels are usually classified according to their primary ionic selectivity. The main groups are Na^+, K^+, and Ca^{2+} channels. While it appears that there is only one type of Na^+ channel, K^+ and Ca^{2+} channels can be further subdivided according to specific biophysical and pharmacological properties. The above-mentioned authors have identified dynamic properties of each ion channel by separating them using different specific chemical blockers.

For example, applying 0.1–40 μM tetrodotoxine (TTX) reversibly blocked the fast component of the action potential, which was probably dominated by I_{Na} (Lipton and Tauck 1987; Kaneda and Kaneko 1991a; Skaliora et al. 1993). When 40 μM TTX and 20 mM tetraethylammonium (TEA) were added together, the depolarizing stimulus elicited a slower action potential followed by a small after-hyperpolarization, which was caused by at least partial blockade of the Na^+ channel, the delayed outward K^+ channel I_K, and the transient K^+channel I_A. I_K and I_A contribute to the repolarization phase of the action potential. Ca^{2+} entering during the action potential activate a K^+ conductance which, along with I_K, contributes to the after-hyperpolarization. This constitutes a negative feedback in which an inward current triggers outward K^+ currents, which can influence the rate at which the cell reaches threshold. It follows that these outward K^+ currents can modulate the spike frequency. $I_{K.Ca}$ underlies the after-hyperpolarization in cat and rat ganglion cells. In whole-cell recordings using patch electrodes (Lipton and Tauck 1987; Kaneda and Kaneko 1991b), I_{Na} and I_{Ca} were isolated by suppressing the outward I_K currents with intracellular Cs^+ and TEA. $CoCl_2$ 3 mM was added to the bath to suppress I_{Ca}, and in the other experiment 1 μM TTX suppressed I_{Na}. The rates of activation and inactivation were slower for the Ca^{2+} than for Na^+ components.

For the purpose of this study, and based on the available data in the literature, we have simulated action potentials using five components: Na^+ current, I_{Na}; Ca^{2+} current, I_{Ca}; a current with properties similar to the delayed outward K^+ current, I_K; a transient A-type K^+ current I_A; and a Ca^{2+}-activated K^+ current, $I_{K.Ca}$.

The basic equation for the spatially uniform membrane potential is:

$$C\frac{dV}{dt} = -F + I \tag{2}$$

where C is the cell capacitance, V the membrane potential, F the membrane current, and I the external current.

For the membrane of cat ganglion cells we describe F on the basis of patch-clamp experiments on solitary rat ganglion cells (Lipton and Tauck 1987) and on cat ganglion cells (Kaneda and Kaneko 1991a,b). The following description of different current channels was based on ideas developed for salamander ganglion cells (Fohlmeister et al. 1990). The experiments on which the simulation of salamander ganglion cells was based were performed at a temperature of 22 °C. Therefore, most of the coefficients describing a_x and b_x (characteristics for each channel) must be adapted with a temperature correction factor Q_{10} to be applicable to cat ganglion cells.

The membrane current F is described by the following set of formulas:

$$F(V, m, h, n, c, A, h_A) = I_{Na} + I_K + I_{Ca} + I_A + I_{K.Ca} \tag{3a}$$

$$I_{Na} = g_{Na} h m^3 (V - V_{Na}) \tag{3b}$$

$$I_K = g_K n^4 (V - V_K) \tag{3c}$$

$$I_{Ca} = g_{Ca} c^3 (V - V_{Ca}) \tag{3d}$$

$$I_A = g_A a^3 h_A (V - V_K) \tag{3e}$$

$$I_{K.Ca} = g_{K.Ca}[Ca]^2/(1 + [Ca]^2)(V - V_K) \tag{3f}$$

$$\frac{d\,Ca}{dt} = -0.000015 I_{Ca} - 0.02([Ca] - 0.0001) \tag{4}$$

$$\frac{dx}{dt} = (x(V) - x_n)/\tau \tag{5a}$$

where $\tau = 1/(a_x + b_x)$ and $x_n = a_x/(a_x + b_x)$ with x denoting the different channels (m, h, n, c, A, h_A), C = 1.0 $\mu F/cm^2$, and g_{Na} = 60.0 mS/cm^2. This conductance was set larger than the standard value because there is a higher density of Na^+ channels in the axon hillock and initial segment (Wollner and Catterall 1986). g_{Ca} = 2.0 ms/cm^2, g_K = 12.0 mS/cm^2, g_A = 36.0 m/cm^2, $g_{K.Ca}$ = 0.05 mS/cm^2, V_{Na} = 35 mV, and V_K = −75 mV. V_{Ca} depends on the intracellular $[Ca^{2+}]$ and was updated from the Nernst equation.

By curve fitting to patch-clamp data from rat ganglion cells, and after temperature coefficient correction (Q_{10}), the following coefficients a_x and b_x were found:

$$a_m = \frac{-0.05(V + 30)}{e^{-0.1(V+30)} - 1} Q_{10} \tag{5b}$$

$$b_m = 0.5 e^{-(V+55)/18} Q_{10} \tag{5c}$$

$$a_h = 0.0182 e^{-(V+50)/20} Q_{10} \tag{5d}$$

$$b_h = \frac{0.35}{e^{-0.1(V+20)} + 1} Q_{10} \tag{5e}$$

$$a_n = \frac{-0.004(V + 40)}{e^{-0.1(V+40)} - 1} Q_{10} \tag{5f}$$

$$b_n = 0.025e^{-(V+50)/80}Q_{10} \tag{5g}$$

$$a_c = \frac{-0.003(V+13)}{e^{-0.1(V+13)}-1}Q_{10} \tag{5h}$$

$$b_c = 0.0467e^{-(V+38)/18}Q_{10} \tag{5i}$$

$$a_A = \frac{-0.0011(V+90)}{e^{-0.1(V+90)}-1}Q_{10} \tag{5j}$$

$$b_A = 0.00667e^{-(V+50)/10}Q_{10} \tag{5k}$$

$$a_{h_A} = 0.105e^{-(V+70)/20}Q_{10} \tag{5l}$$

$$b_{h_A} = \frac{0.1}{e^{-0.1(V+40)}+1}Q_{10} \tag{5m}$$

The parameter space for (2)–(5), describing retinal ganglion cell properties, has a very large dimension, and many complex bifurcations can probably be found. An interesting example is the influence of extracellular $[Ca^{2+}]$ on the dynamic membrane properties of the K^+ channel, as was shown for pancreas cells by Rinzel and Lee (1986). Because pancreas cells have only a slow Ca^{2+} activation, a small change in the extracellular $[Ca^{2+}]$ has a strong influence on their spike generation properties.

We integrated (2), (3), (4) and (5) (that were based on fitted patch-clamp data) and adjusted some of the coefficients to obtain the proper shape of the action potentials in our ganglion cell recording. An example of the comparison between simulated action potentials and 20 superimposed spikes of the X-type cat ganglion cell is shown in Fig. 2. It can be seen that the equations accurately describe the shape of the measured spikes. All coefficients of the function F found in this way were subsequently fixed and not changed in further simulations. Therefore, the complexity of the equations describing spike generation did not increase the degrees of freedom in the final fits. We performed a similar analysis for other intracellularly recorded ganglion cells. The shape of action potentials, and hence the coefficients describing them, were mostly very similar, although there was some variation in the duration of action potentials.

In cat retinal ganglion cells, activation is caused not only by a slow Ca^{2+} channel as in pancreas cells, but mainly through a fast Na^+ channel. This fact has important consequences. In case the Na^+ channel is blocked, the change from non-oscillatory (a fixed point) to oscillatory (a limit cycle) behavior can be caused by only a 20% change in extracellular $[Ca^{2+}]$, similar to pancreas cells (Rinzel and Lee 1986). When the Na^+ channel is opened, sensitivity to extracellular $[Ca^{2+}]$ is significantly decreased, and an increase by a factor of 200 is needed to change membrane properties from non-oscillatory to oscillatory at the same depolarizing current. This phenomenon is an example of the stabilizing effect of channel interactions. It shows that for the simulation of spike generation, we have to take the actual complexity of channel interactions into account.

2.4 Coupling between the membrane and generator potential oscillators

To simulate spike generation of ganglion cells, a strong coupling between the van der Pol oscillator and the Hodgkin-Huxley equations must be considered. The generator potential forces the membrane"s nonlinear oscillator to change its state, which through a Hopf bifurcation may produce action potentials. Action potentials are generated in the axon hillock where there is a high density of voltage-gated Na^+ channels (Wollner and Catterall 1986) and thus the lowest threshold. Generated action potentials spread in two directions: along the axon to higher centers of the brain, and in the opposite direction, through the cell body and to its dendritic tree (Carras et al. 1992; Carras and Miller 1987). This retrograde activity (spreading back) causes an increase in the threshold for postsynaptic potentials. Therefore, the generator potential not only acts as an external force for spike generation, but is also affected by the generated spikes.

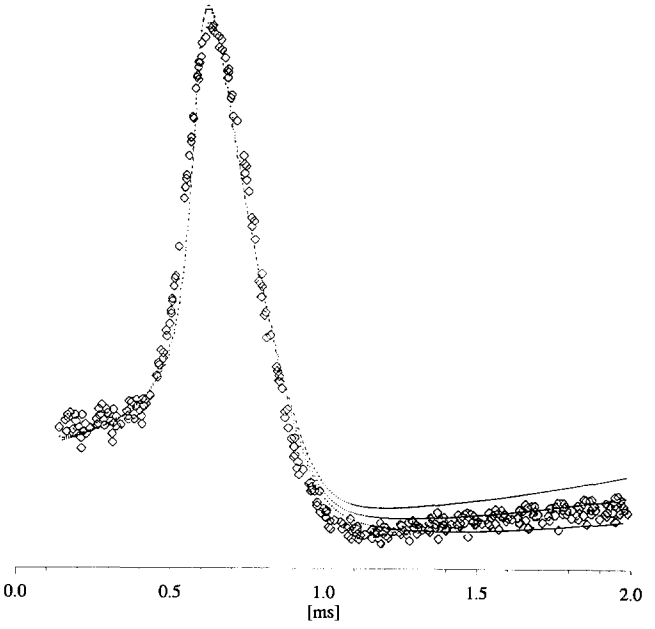

Fig. 2. Simulation results (*dotted curves*) obtained from integration of (6), (7) and (8) for three different depolarization currents (10, 20, 30 $\mu A/cm^2$) compared with experimental data (*large diamonds*). Experimental data consist of 20 subsequent spikes at different depolarization levels. The sampling frequency of the experimental data was 10 kHz. The integration step size for the simulations was 15 μs

This interaction can be simulated by coupling, through a negative feedback, the slow G-potential oscillator to the much faster oscillator representing ganglion cell membrane properties. In such a model, one must consider not only the phase but also the amplitude of both oscillations to explain effects such as dying out of the fast oscillations (Aronson et al. 1990; Przybyszewski et al. 1993; e.g., Fig. 1 for 24 Hz).

The coupled oscillators can be described as:

$$\frac{dx}{dt} = k(y + x - x^3/3 - g_2V_{th} + \text{dep}) \tag{6a}$$

$$\frac{dy}{dt} = 1/k(-x + a + b\cos(\omega t/600)) \tag{6b}$$

$$C\frac{dV}{dt} = -F + g_1x \tag{6c}$$

where the coefficients g_1 and g_2 describe the coupling between the oscillators. g_1 represents the external membrane

Table 1. The values of model parameters used to simulate the experimental results. Only the parameters that were changed to reproduce the findings for different spot sizes and stimulus frequencies (stim. freq.) are shown. Other parameter values are given in the text

Stim. freq.	Spot size (deg)	a	b	k	g_1	g_2	dep
2 Hz	0.7	-0.35	0.8	8	0.35	1.53	2.1
	0.5	-0.35	0.8	8	0.52	1.64	2.1
	0.2	-0.35	0.8	8	1.2	2.2	2.1
4 Hz	0.7	-0.35	0.8	10	0.48	1.45	2.1
	0.5	-0.35	0.8	10	0.56	2.1	2.1
	0.2	-0.35	0.8	10	1.18	2.14	2.1
8 Hz	0.7	-1.67	1.75	16	0.4	5.9	12.7
	0.5	-1.67	1.75	16	0.55	5.9	12.7
	0.2	-1.67	1.75	16	1.2	6.0	12.7
16 Hz	0.7	-1.67	1.75	8	1.0	6.0	12.7
	0.5	-1.67	1.3	8	1.2	6.0	11.7
	0.2	-1.67	1.04	8	1.2	6.0	10.92

current caused by the generator potential, and g_2 describes the strength of negative feedback from the action potential (V_{th} value of the membrane potential above threshold) to the generator potential; dep is a DC shift of the intracellular potential. Depending on the position of the synapse on the cell body or the dendritic tree, the values of g_1 and g_2 can change, consequently changing the mode of oscillation (Przybyszewski et al. 1995).

Figure 3 shows traces of the experimental responses, together with fitted model simulations. Figure 1 provides a quantitative summary of the spike train responses in these recordings. To reproduce the presented experimental data, the parameters were chosen at first to simulate the most regular bursting observed for a stimulation frequency of 8 Hz and a spot size of 0.7 deg (see Figs. 1, 3). In the next step, the stimulation frequency was changed and the van der Pol oscillator was decoupled to generate changes as described in our previous work (Przybyszewski et al. 1993). After recoupling both oscillators, the coefficient of nonlinearity, k, of the van der Pol oscillator was increased. As in our previous simulations, k was highest for a stimulation frequency of 8 Hz and decreased for the lower and higher light stimulus frequencies (Table 1). The other coefficients in the van der Pol oscillator were also adjusted to simulate the characteristic changes with stimulus frequency. Changes in spot size could be simulated by changing only the coupling coefficients g_1 and g_2 (except for a frequency of 16 Hz: see Table 1).

The parameters in Table 1 are related to the properties of the van der Pol oscillator, the coupling between both oscillators and ganglion cell depolarization. Threshold coefficient a, forcing amplitude b, nonlinearity k, feedback coupling g_2 and depolarization (dep) strongly depend on the stimulus frequency. The values of a, b, g_2 and dep fall into two groups: a first group for 2 and 4 Hz, and a second group for 8 and 16 Hz. This could indicate that different processes underlie the response dynamics for low (2, 4 Hz) or high stimulus frequencies (8, 16 Hz). The coefficient of nonlinearity k, also shows a strong dependence on stimulus frequency. It is highest at a frequency of 8 Hz, which is the most nonlinear case, with regular spike bursting. Similar changes were observed in the power spectra of the generator potential (Przybyszewski et al. 1993), where the number of harmonics increased with stimulus frequency up to 8 Hz and then decreased for still higher temporal frequencies. A stimulus frequency of 8 Hz obviously has special meaning. The relaxation character of the oscillations around 8 Hz ameliorates and accelerates synchronization between the different oscillators (Somers and Kopell 1993).

The change in spot size is most strongly correlated to the feedforward coupling coefficient g_1. The increase in g_1 with decreasing spot size might be related to the weight of synapses, which will be larger when a synapse is closer to the cell body. Synapses near the cell body should also give a larger back-coupling coefficient g_2. This is supported by the results for lower stimulus frequencies (2, 4 Hz). These observations are in agreement with a Gaussian shape of the ganglion cell receptive field center.

Quantitative and qualitative comparisons of simulated ganglion cell responses and experimental results are shown in Figs. 1 and 3. It can be seen that the final model accurately reproduces the many different response patterns. Simulation of very short bursts, as observed for a stimulus frequency of 8 Hz (spot sizes 0.5 and 0.7 deg), appeared most critical. Other types of bursting were simulated fairly well (Figs. 1A, 3). The model could also reproduce the different types of irregularities in the spike bursts (Fig. 1C, 3).

3 Discussion

3.1 Simulation of active membrane properties

Hodgkin and Huxley (1952), in their famous paper, described and simulated action potential generation in the squid axon by a transient inward Na^+ current followed by an outward K^+ current. On the basis of these early studies, it was assumed that complex brain functions could be related to the connectivity between simple neural cells that were electrophysiologically similar to the squid axon (and motoneurons). In recent years, however, the development of patch-clamp, immunological, and molecular biological techniques has demonstrated many different voltage- and ligand-dependent ionic conductances in cell membranes of the mammalian central nervous system (Llinas 1988). A variety of so-called low-threshold Ca^{2+} channels and up to 12 varieties of outward K^+ currents have been found (for review see Llinas 1988). Other types of complexity are seen in computer simulation studies, showing that even simple and uniform membrane properties, such as those of the squid axon, could lead to complex spike patterns. Aihara et al. (1984), for example, found synchronization, quasi-periodic, and chaotic oscillations in both experiments on, and computer simulation of, a squid giant axon. From a theoretical point of view, "simple" Hodgkin-Huxley equations are too complex for a general analytical solution, and only some periodic solutions (different types of burst patterns) were classified (e.g. Carpenter 1979). Intracellular recordings and patch-clamp studies in retinal ganglion cells (Kaneda and Kaneko 1991a,b; Lipton and Tauck 1987; Lukasiewicz and Werblin 1988; Skaliora et al. 1993) show that their membrane properties are much more complex than those found in the squid axon. We have approximated cat ganglion cell membrane properties by eighth-order nonlinear differential equations similar to those proposed by Fohlmeister et al.

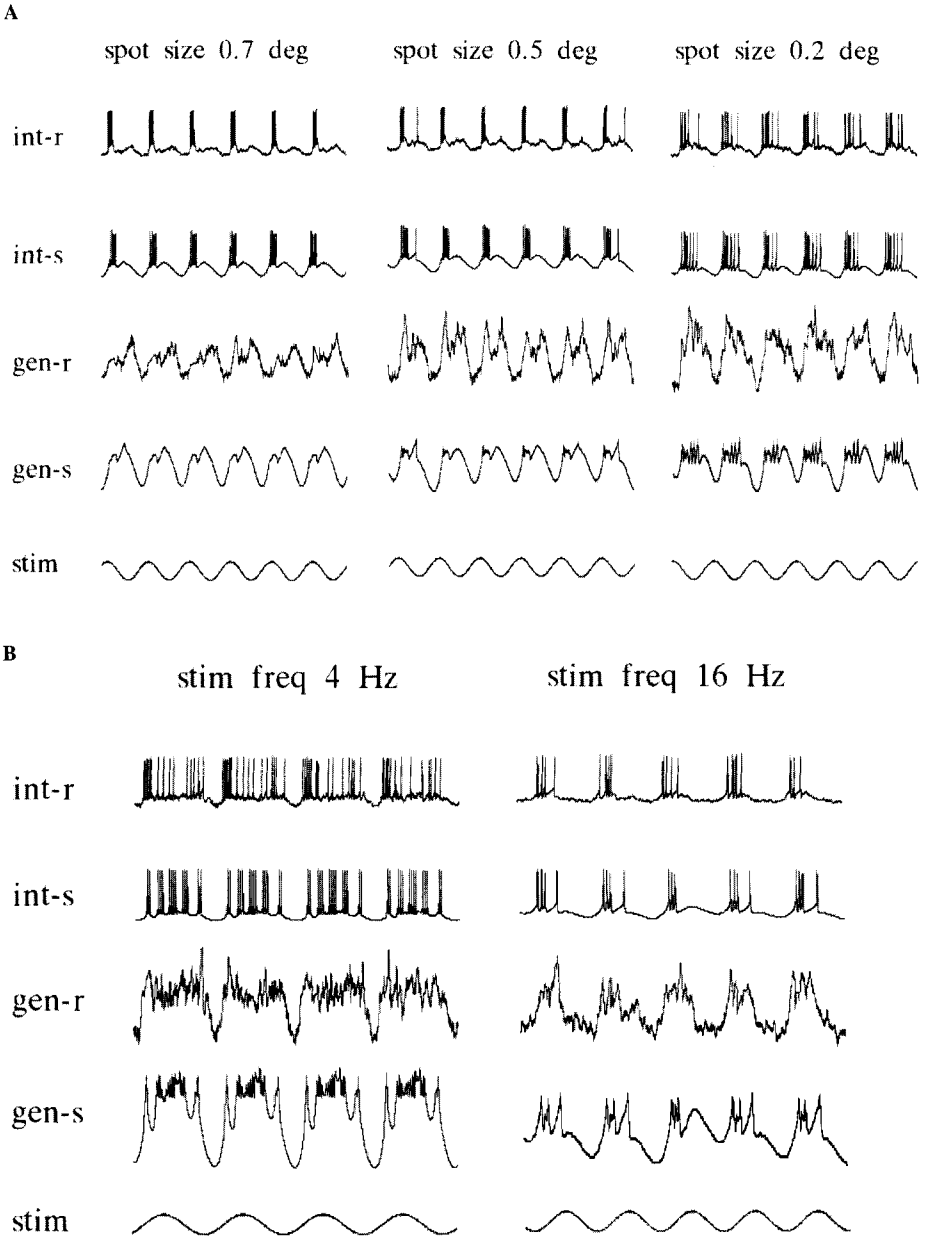

Fig. 3A,B. Experimental and simulated results compared for the ganglion cell of Fig. 1. **A** Recorded (r) and simulated results (s) for a stimulus frequency of 8 Hz. Spot sizes in degrees are indicated in the figure. **B** Recorded (r) and simulated (s) responses for a spot size of 0.7 deg and stimulus frequencies 4 and 16 Hz. The *top two traces* show the intracellular potential (*int*); the *middle traces* represent recorded and simulated spike-free generator potentials (*gen*); and the *bottom traces* represent the sinusoidal intensity modulation

(1990) for salamander ganglion cells. Our parameters describing the active membrane properties (5b) to (5m), are different due to differences in the body temperature between cat and salamander. We noticed, furthermore, that different cells may have action potentials with different shapes. This could be caused by different electrode positions in the ganglion cell and/or different channel properties. An example of the latter is the heterogeneity of different K^+ channels, which arises in part from the large number of genes encoding different subunits and also from the assembly of different subunits into heteromultimetric channels (e.g., Sheng et al. 1993). Recently a new K^+ channel with slower dynamics was found in newborn rat solitary ganglion cells (Sucher and Lipton 1992). Villa and Blanco (1994) suggested that the contribution of different K^+ channels is a crucial factor in determining the spike pattern, and that it could, for example, determine differences between X- and Y-type ganglion cell spiking patterns. It seems, however, that there are differences in the membrane properties between adult cats and newborn rats. For example, the Ca^{2+} channel in cats is identical to the high-threshold (L-type) channel (Kaneda and Kaneko 1991b) whereas in postnatal retinal ganglion cells in rats the low-threshold, transient (T-type) Ca^{2+} channel also exists (Karschin and Lipton 1989).

Given the complexity of the many different types of ion channels, and their interactions, it is obvious that our model, which takes six different ion currents into account, can provide only a first-order description of the active membrane properties of cat retinal ganglion cells. The description is, however, realistic enough to account for the observed spike dynamics (Fig. 3), and for many of the previously described membrane properties. Our description consists of an eighth-order differential equation, but it should be noted that all its parameters were fixed in the final simulations. Differences in spike patterns for different temporal frequencies and for different spot sizes were accounted for by changing the state

of the van der Pol oscillator and its coupling to spike generation.

3.2 Coupling between generator potential and active membrane properties

In our model, spike train activity of a ganglion cell was simulated by coupling the generator potential and the membrane properties, both of which can be described as oscillators. The van der Pol oscillator describes the generator potential fluctuations, and the integrated Hodgkin-Huxley equations describe the active membrane oscillator. In this approach it is assumed that the input current exciting the membrane at the axon hillock is proportional to the generator potential. Evidence from immunocytochemical techniques point to a high density of Na^+ channels in axon hillocks and axon initial segments in the ganglion cell of adult frog and rat retina (Wollner and Catterall 1986). There is also evidence from other electrophysiological and computer simulation studies that the spike begins in the initial axon segment and spreads back into the soma as well as down the axon (Miller 1986; Carras and Miller 1987; Carras et al. 1992). This retrograde activity (back propagation to the dendrites) forms the biophysical basis for the feedback coupling in our model.

It is important to notice that this type of coupling will not perturb the limit cycles of the individual oscillators. The character of the membrane depolarization will be determined by its inherent properties and not by the strength of the coupling. This kind of coupling will influence the phase of oscillation without changing internal properties of the oscillators (Grasman 1987).

We have shown previously (Przybyszewski et al. 1995) that, for a simple case when the membrane properties were modeled by the Bonhoeffer–van der Pol oscillator (after FitzHugh 1955), a change in the coupling coefficient (related to spike back-propagation) can lead to a change in the spike train pattern. Furthermore, a change in the coupling strength between two such oscillators could also change the "presynaptic" oscillations. Generator-potential oscillations could thus be changed from chaotic to periodic and vice versa (Przybyszewski et al. 1995). Such observations are not too surprising, because many complicated processes have been observed by coupling two or more oscillators with similar nonlinear properties (Linsay and Cumming 1989; Baesens et al. 1991; Aronson et al. 1992). In the present paper we have shown that similar interactions can be accounted for if we use a biophysically realistic description of the active membrane properties, based on Hodgkin–Huxley equations. Furthermore, a realistic spike generator allows us to study the relation between oscillations in the generator potential and in the spike train in much more detail.

3.3 Oscillations in the generator potential and in the spike train

A sinusoidal stimulus induces two kinds of change in the ganglion cell's state: a component that follows the stimulus and, superimposed on this, fast oscillations. The slow component is related to bursting in each period of light stimulation, whereas the fast oscillations are related to changes within bursts. Such fast oscillations within bursts generally do not survive signal averaging, and were therefore considered as noise in intraretinal processing. Consequently, it was assumed that the information was carried only by the mean spike frequency. We have shown that this "noise" can also be described as complex oscillations that depend on both stimulus parameters and retinal properties (Przybyszewski et al. 1993). The fast oscillations might, therefore, also carry relevant information. Similar fast, oscillatory behavior has been observed in many parts of the visual cortex and it has been suggested that it plays an important role in visual perception (Singer 1993; Frien et al. 1994). One purpose of the present analysis was to investigate the possible sources of the oscillations that show up in spike trains. In our experiments the mean number of spikes in each burst did not depend on spot size, and the mean spike frequency was largely independent of stimulation frequency (Fig. 1D). Also, the phase shift (delay) between stimulus and response did not depend on spot size (Fig. 1B). Yet, the different stimuli could clearly be distinguished if the spike patterns and their irregularities were taken into account. We showed that the relative burst duration and irregularity substantially change with flicker frequency and spot size (Fig. 1A,C). Some of these changes result directly from the oscillations observed in the generator potential and are presumably driven by intraretinal activity. Other types of oscillation resulted from interactions between the two oscillators, and could be changed by changing the coupling strength. Most of these oscillations could either be synchronized to the stimulus or non-synchronized. The present analysis of intracellular ganglion cell responses indicates that spike train oscillations are similar to those in the generator potential. This indicates that the irregular behavior in spike bursting may very well result from a deterministic process, simulated by the coupling of two oscillators. The inverse effect can occur where, for example, chaotic oscillations in the G-potential are stabilized by the spike generating mechanism [e.g., Rajasekar and Laksmann (1991) investigated the possibilities of controlling chaos in a Bonhoeffer–van der Pol oscillator]. Such interactions might explain why the variability (noise) in spike trains in the lateral geniculate nucleus LGN is lower than that in the retina (Levine 1994; Mukherjee et al. 1994).

In conclusion, regular versus irregular spike patterns and synchronized versus non-synchronized patterns may transmit intraretinal information to higher visual centers that cannot be recovered in averaged responses. Modeling of these real-time response properties increases our knowledge about transmission of visual information, and coding of information in general.

Acknowledgements. We thank Paolo Gaudiano for his comments on and improvements of the manuscript, and Cindy Bradford and Michael Yeh for improvements in the English. A.W.P. thanks Prof. K.D. Schotte (Physics Dept. FU) and Prof. B. Fiedler (Math. Dept. FU) for their help and for the use of their Sun Workstations, and Laura Giannitrapani for help with figures. A.W.P. was supported by Whitehall Foundation grant S93-24.

References

Aguirre LA, Billings SA (1994) Validating identified nonlinear models with chaotic dynamics. Int J Bifurcation and Chaos 4: 109–125

Aihara K, Matsumoto G, Ikegaya Y (1984) Periodic and non-periodic responses of a periodically forced Hudgkin-Huxley oscillator. J Theor Biol 109: 249–269

Aronson DG, Ermentrout GB, Kopell N (1990) Amplitude response of coupled oscillators. Physica D 41: 403-449

Back A, Guckenheimer J, Myers M, Wicklin F, Worfolk P (1992) Dstool: computer assisted exploration of dynamical systems. Notices Am Math Soc 39: 303–309

Baesens C, Guckenheimer J, Kim S, MacKay RS (1991) Three coupled oscillators: mode-locking, global bifurcations and toroidal chaos. Physica D 49: 387–475

Baird B (1986) Nonlinear dynamics of pattern formation and pattern recognition in the rabbit olfactory bulb. Physica D 22: 150–175

Boer E de, Kuyper P (1968) Triggered correlation. IEEE Trans Biomed Eng 15: 169–175

Braaksma B (1993) Critical phenomena in dynamical systems of van der Pol type. PhD thesis, Utrecht University

Carpenter GA (1979) Bursting phenomena in excitable membranes. SIAM J Appl Math 36: 334–372

Carras PL, Miller RF (1987) The role of axon's initial segment and thin region in the initiation of ganglion cell impulses. Invest Ophthalmol Vis Sci 28 [Suppl]: 406

Carras PL, Coleman PA, Miller RF (1992) Site of action potential initiation in amphibian retinal ganglion cells. J Neurophysiol 67: 292–304

Enroth-Cugell C, Robson JG (1966) The contrast sensitivity of retinal ganglion cells of the cat. J Physiol (Lond) 187: 517–552

FitzHugh R (1955) Mathematical models of threshold phenomena in the nerve membrane. Bull Math Biophys 17: 257–278

Fohlmeister JF, Coleman PA, Miller RF (1990) Modeling the repetitive firing of retinal ganglion cells. Brain Res 510: 342–345

Freeman WJ (1987) Simulation of chaotic eeg patterns with a dynamic model of the olfactory system. Biol Cybern 56: 139–150

Frien A, Eckhorn R, Bauer R, Woelbern T, Kehr H (1994) Stimulus-specific fast oscillations at zero phase between visual areas V1 and V2 of awake monkey. Neuroreport 5: 2273–2277

Grasman J (1987) Asymptotic methods for the relaxation oscillations and applications. Springer, Berlin Heidelberg New York

Grind WA van de (1981) Intracellular recording studies of visual signal processing in the cat retina. Doc Ophthalmol Proc Ser 30: 21–30

Hodgkin AL, Huxley AF (1952) A quantitative description of membrane current and its application to conduction and excitation in nerve. J Physiol (Lond) 117: 500–544

Honerkamp J, Mutscher G, Seitz R (1985) Coupling of a slow and a fast oscillator can generate bursting. Bull Math Biol 47: 1–21

Kaneda M, Kaneko A (1991a) Voltage-gated sodium currents in isolated retinal ganglion cells of the cat: relation between the inactivation kinetics and the cell type. Neurosci Res 11: 261–275

Kaneda M, Kaneko A (1991b) Voltage-gated calcium currents in isolated retinal ganglion cells of the cat. Jpn J Physiol 41: 35–48

Karschin A, Lipton SA (1989) Calcium channels in solitary retinal ganglion cells from post-natal rat. J Physiol (Lond) 418: 379–396

Lankheet MJM, Molenaar J, Grind WA van de (1989) The spike generation mechanism of cat retinal ganglion cells. Vision Res 29: 505–517

Levine MW (1994) Transfer of information and tailored variability in the dorsal lateral geniculate nucleus of cat. Invest Ophthalmol Vis Sci 35 [Suppl]: 1975

Linsay PS, Cumming AW (1989) Three-frequency quasiperiodicity, phase locking, and the onset of chaos. Physica D 40: 196–217

Lipton SA, Tauck DL (1987) Voltage-dependent conductances of solitary ganglion cells dissociated from the rat retina. J Physiol (Lond) 385: 361–391

Llinas RR (1988) The intrinsic electrophysiological properties of mammalian neurons: insight into central nervous system function. Science 242: 1654–1664

Lukasiewicz P, Werblin F (1988) A slow inactivating potassium current truncates spike activity in ganglion cells of the tiger salamander retina. J Neurosci 8: 4470–4481

Miller RF (1986) Impulse initiation in retinal ganglion cells. Invest Ophthalmol Vis Sci 27 [Suppl]: 171

Mukherjee P, Sanchez-Vives M, Reich DS, Kaplan E (1994) A comparison of the response variability of neurons in the cat LGN with that of their retinal input. Invest Opthalmol Vis Sci 35 [Suppl]: 1975

Przybyszewski AW (1991) An analysis of the oscillatory patterns in the central nervous system with the wavelet method. J Neurosci Methods 38: 247–257

Przybyszewski AW, Lankheet MJM, Grind WA van de (1993) Oscillations of the generator potential in X retinal ganglion cells of cat. Vision Res 33: 861-875

Przybyszewski AW, Lankheet MJM, Grind WA van de (1995) Irregularities in spike train of cat retinal ganglion cells. In: Proc 2nd conference on experimental chaos. Dito W, Pecora L, Vohra S, Shlesinger M, Spano M (eds) World Scientific, Singapore New Jersey London Hong Kong, pp. 218–225

Rajasekar S, Laksmann M (1991) Controlling of chaos in Bonhoeffer-van der Pol oscillator. Int J Bifurcation and Chaos 2: 201-204

Rinzel J, Lee YS (1986) On different mechanisms for membrane potential bursting. In: Othmer HG (ed.) Nonlinear oscillations in biology and chemistry. Springer, Berlin Heidelberg New York, pp. 19–33

Villa P, Blanco R (1994) Modelling the transient/sustained firing of retinal ganglion cells. Invest Ophthalmol Vis Sci 35 [Suppl]: 2124

Wilson HR, Cowan JD (1972) Excitatory and inhibitory interactions in localized populations of model neurons. Biophys J 12: 1–13

Sheng M, Liao YJ, Jan YN, Jan LY (1993) Presynaptic A-current based on heteromultimeric K^+ channels detected in vivo. Nature 365: 72–75

Singer W (1993) Synchronization of cortical activity and its putative role in information processing and learining. Annu Rev Physiol 55: 349-374

Skaliora I, Scobey RP, Chalupa LM (1993) Prenatal development of excitability in cat retinal ganglion cells: action potentials and sodium currents. J Neurosci 13: 313–323

Sucher NJ, Lipton SA (1992) A slowly inactivating K^+ current in retinal ganglion cells from postnatal rat. Vis Neurosci 8: 171–176

Somers D, Kopell N (1993) Rapid synchronization through fast threshold modulation. Biol Cybern 68: 393–407

Wollner DA, Catterall WA (1986) Localization of sodium channels in axon hillocks and initial segments of retinal ganglion cells. Proc Natl Acad Sci USA 83: 8424–8428